Journal of Magnetism and Magnetic Materials 509 (2020) 166895

Contents lists available at ScienceDirect

Journal of Magnetism and Magnetic Materials

journal homepage: www.elsevier.com/locate/jmmm

Research articles

Switching of skyrmioniums induced by oscillating magnetic field pulses

H. Vigo-Cotrina[a,*], A.P. Guimarães[a]

[a] Centro Brasileiro de Pesquisas Físicas, 22290-180 Rio de Janeiro, RJ, Brazil

ARTICLE INFO

Keywords:
Skyrmionium
Target skyrmion
Switching skyrmionium
Micromagnetic simulation

ABSTRACT

Skyrmioniums are exotic magnetic configurations that have several potential applications, as devices for magnetic recording, in Spintronics. In this work, using micromagnetic simulation, we show that it is possible to switch a skyrmionium in an isolated nanodisk. First, we have obtained the ground state of the nanodisk for a fixed value of perpendicular anisotropy constant K_z and for several values of Dzyaloshinskii-Moriya exchange constant D_{int}. Next, in order to obtain the frequencies of the spin wave mode, we have calculated the power spectrum of the fluctuations of the spatial z-component of the magnetization for values of D_{int} where the ground state of nanodisk is a skyrmionium. Our results show that applying oscillating perpendicular magnetic field pulses with a frequency equal to that of the spin wave mode, and tuning the values of the intensity of the applied magnetic field and its duration in the sub-nanosecond range, one can switch the polarity of the skyrmionium in the nanodisk. We have also obtained, from the micromagnetic simulation of the process of inversion of polarity of the skyrmioniums, the several intermediate magnetic configurations of the nanodisk, revealing the full complexity of this phenomenon.

1. Introduction

Several exotic spin textures can be obtained in magnetic nanodisks, e.g., circular vortices [1–3], radial vortices [4–6], skyrmions [7–12] and skyrmioniums (also called target skyrmions) [13–18].

Of this group of exotic magnetic configurations, due to their small size and topological protection, skyrmions and skyrmioniums have gained interest in recent years [7–11,13–17,18,19]. These magnetic configurations were predicted and studied theoretically by Bogdanov et al. [20]. The spatial profile of a skyrmion is characterized by two out-of-plane domains separated by an in-plane domain wall [21]. The inner out-of-plane domain is called the core of the skyrmion [7,10,21], and has polarity $p = +1$, when the core points along the $+z$ direction, and $p = -1$ in the $-z$ direction [7,10,11]. The outer out-of-plane domain always has a direction opposite to that of the core [21].

Unlike the skyrmion, the spatial profile of a skyrmionium has an additional outer out-of-plane domain. This domain has the same direction of the magnetization of the core [13–18]. Therefore, a skyrmionium can be considered a combination of two skyrmions with opposite topological charges ($Q = +1$ and $Q = -1$), resulting in a total topological charge $Q = 0$ [16,22].

The dynamics of skyrmions and skyrmioniums can be induced by the application of an external perturbation, e.g., a spin polarized current [8,13,23] or a magnetic field pulse [16,24].

One of the advantages of using skyrmioniums instead of skyrmions is that skyrmioniums have a topological charge $Q = 0$, allowing them to move without suffering deflections due to the skyrmion Hall effect (SkHE) [25,26].

Another advantage of the skyrmioniums is that they can reach higher velocities in comparison with the skyrmions [25]. Skyrmions and skyrmioniums have potential applications in devices for magnetic recording [23,26–29]. In these potential applications, a skyrmionium with polarity $p = +1$ could store the bit information 1 (or 0) and a skyrmionium with polarity $p = -1$, could store the bit information 0 (or 1). Thus, it is important to find a mechanism to switch between 1 and 0.

Although the issue of switching is well studied in the case of skyrmions [30–34], it is still necessary to find new methods to perform the switching in the case of skyrmioniums. With this in mind, we have studied the switching process of a skyrmionium in an isolated nanodisk, when one applies oscillating perpendicular magnetic fields. For this purpose, we used the GPU-accelerated micromagnetic simulation software MuMax3 [35]. The nanodisk was discretized in small $1 \times 1 \times L$ nm^3 size cells, where L is the thickness of the nanodisk. The material used was Cobalt, with typical parameters [7,35]: saturation magnetization $M_s = 5.8 \times 10^5$ A/m, exchange stiffness $A_{ex} = 15$ pJ/m. We assumed $T = 0$ K, however, the present method is valid at room temperature (see Supplementary Material).

* Corresponding author.
E-mail address: vigohel@outlook.com (H. Vigo-Cotrina).

https://doi.org/10.1016/j.jmmm.2020.166895
Received 13 February 2020; Received in revised form 7 April 2020; Accepted 11 April 2020
Available online 18 April 2020
0304-8853/ © 2020 Elsevier B.V. All rights reserved.

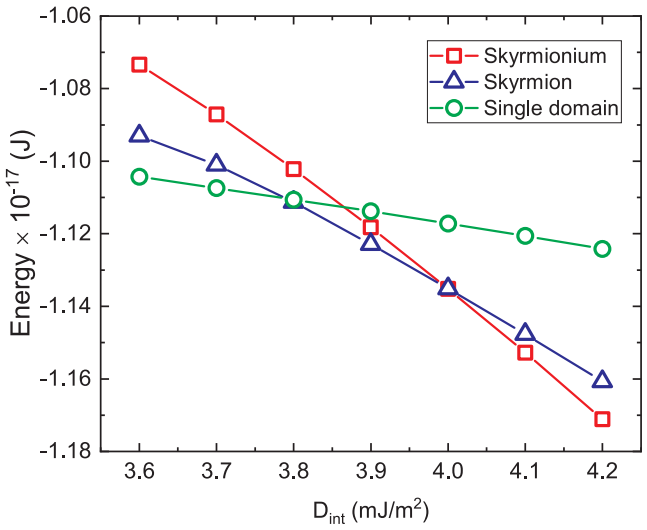

Fig. 1. Energy of the final magnetic states of the nanodisk versus value of the Dzyaloshinskii-Moriya exchange constant D_{int}.

2. Results and discussion

We considered a Co nanodisk coupled to a nonmagnetic substrate, having a diameter D = 150 nm and a thickness L = 1 nm. We have chosen a fixed value of perpendicular uniaxial anisotropy constant $K_z = 0.8$ MJ/m^3; the Dzyaloshinskii-Moriya exchange constant D_{int} was varied from $D_{int} = 3.6$ to $D_{int} = 4.2$ mJ/m^2 in 0.1 mJ/m^2 steps.

In order to obtain the ground state of the nanodisk, we have considered three different initial magnetic configurations: skyrmionium, skyrmion and single domain. In Fig. 1 are shown the energies for the final magnetic states. In all cases, the final magnetic states were the same as the initial states.

In Fig. 1 we can see that for values of D_{int} between 3.6 mJ/m^2 and 3.7 mJ/m^2, the magnetic single domain is the state of lowest energy. For $D_{int} = 3.8$ mJ/m^2, the configuration may be single-domain or skyrmion. For $D_{int} = 3.9$ mJ/m^2, the skyrmion configuration has the lowest energy, and for values of $D_{int} = 4.1$ mJ/m^2 to $D_{int} = 4.2$ mJ/m^2 the skyrmionium configuration is the ground state; for $D_{int} = 4.0$ mJ/m^2 the ground state may be a skyrmion or a skyrmionium.[1]

In order to excite the spin wave modes, we took a skyrmionium in the nanodisk as the initial magnetic state. Next, we have applied a perpendicular sinc magnetic pulse field $B_z = B_0 \mathrm{Sinc}(2\pi f(t-t_0))$, where $t_0 = 1$ ns, $B_0 = 5$ mT is the magnetic field amplitude, and f = 50 GHz is the cutoff frequency.[2] In this stage, we have used a damping constant $\alpha = 0.002$. The spatial profile of the z-component of the magnetization was saved every 5 ps. Following the methodology of Kim et al. [11], we have obtained the power spectrum $S(\omega)$, defined by:

$$S(\omega) = |\int e^{-i\omega t}\delta m_z(t)|^2, \quad (1)$$

where δm_z (t) = m_z(t) - $m_{z,0}$ are the fluctuations of the spatial z-component of the magnetization [11], obtained in the previous stage.

The power spectra S(ω) for different values of D_{int} are shown in Fig. 2. In this Figure, we can see four prominent peaks for each value of D_{int}. These peaks correspond to frequencies of the spin wave modes (mode 1, ···, mode 4).

For $D_{int} = 4.0$ mJ/m^2, the values of the frequencies of the spin wave mode are: f = 2.65 GHz (mode 1), f = 5.70 GHz (mode 2), f = 11.10 GHz (mode 3), f = 22.14 GHz (mode 4) and f = 67.63 GHz (mode 5). For $D_{int} = 4.1$ mJ/m^2, f = 2.75 GHz (mode 1), f = 6.10 GHz (mode 2), f = 11.95 GHz (mode 3) and f = 23.84 GHz (mode 4). For $D_{int} = 4.2$ mJ/m^2, f = 2.85 GHz (mode 1), f = 6.55 GHz (mode 2), f = 12.90 GHz (mode 3) and f = 25.74 GHz (mode 4).

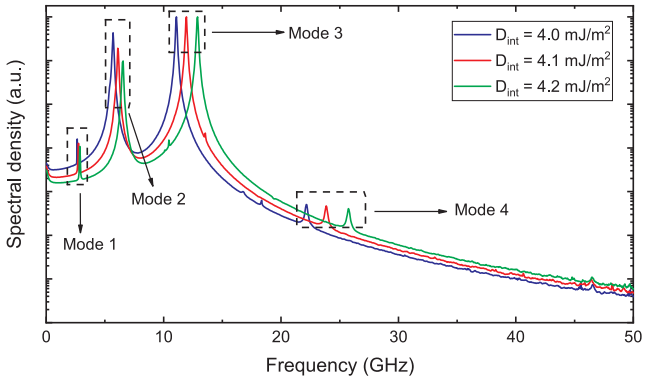

Fig. 2. Power spectra for different values of D_{int}, obtained by fast Fourier transform from the fluctuations of the z-component of the magnetization δ m_z(t). Blue line corresponds to $D_{int} = 4.0$ mJ/m^2, red line to $D_{int} = 4.1$ mJ/m^2 and green line to $D_{int} = 4.2$ mJ/m^2.

As shown in Fig. 2, increasing the value of D_{int}, increases the frequencies of the spin wave modes. An increase of D_{int} also modifies the spatial distribution of the magnetic modes in the nanodisk, therefore a change in the frequencies of the spin wave modes is also expected.

The spatial distribution of FFT power of the spin wave modes is shown in Fig. 3. In this Figure, we can see that all modes, except mode 1, have circular symmetry and the FFT power is distributed both in the region near the center of the nanodisk, and on its edge, being more intense in the central region of the nanodisk.[3]

For all values of D_{int} used in this work, the FFT power of mode 1 is always distributed on the edges of the nanodisk.

Although mode 1, mode 2 and mode 3 have similar spatial distributions, there are differences between them. For example, for $D_{int} = 4.0$ mJ/m^2 (Fig. 3 (a)), mode 2 is more intense on the edge of the nanodisk in comparison to mode 3 and mode 4. Additionally, there is a small decrease in the intensity on the edges of the nanodisk for mode 3 and mode 4 in comparison to mode 2. A similar behavior is observed for $D_{int} = 4.1$ mJ/m^2 (Fig. 3 (b)).

For $D_{int} = 4.2$ mJ/m^2 (Fig. 3 (c)), mode 3 has higher intensity on the edge of the nanodisk, in comparison to mode 2 and mode 4. However, this difference is not as pronounced as in the cases for $D_{int} = 4.0$ mJ/m^2 and $D_{int} = 4.1$ mJ/m^2.

Next, in order to induce switching of the skyrmionium in the nanodisk, we have used an oscillating perpendicular magnetic field $B_z = -B_0 \sin(2\pi ft)$, where B_0 is the magnetic field intensity, and f is the frequency of the spin wave modes previously obtained.[4] In this stage, we have used a value of damping constant[5] $\alpha = 0.01$. In all the simulations, we have considered as the initial magnetic configuration, a skyrmionium with polarity p = +1.

The spatial evolution of the magnetization with time, and the temporal evolution of the average z-component of the magnetization m_z, and the field B_z are shown in Fig. 4 (a-l) and Fig. 4 (m). In Fig. 4 (a-l), we can see how the spatial distribution of the magnetization changes with time for mode 1 during the switching process, from a skyrmionium

[1] We have worked with the region where the skyrmionium is the ground state (4.0 mJ/m^2 ⩽ D_{int} ⩽ 4.2 mJ/m^2).

[2] This pulse allows exciting all spin wave frequencies present in the system up to a value of f = 50 GHz [13,11].

[3] Note that the outer circles coincide with the limits of the nanodisk.

[4] We have shown only the results for $D_{int} = 4.0$ mJ/m^2.

[5] We have used a lower damping constant in order to observe more easily the dynamics of switching. However, we have also used a realistic damping $\alpha = 0.5$ [7]. Our results show that the switching is still possible, but an increase in the values of B_0 is required (see Supplementary Material).

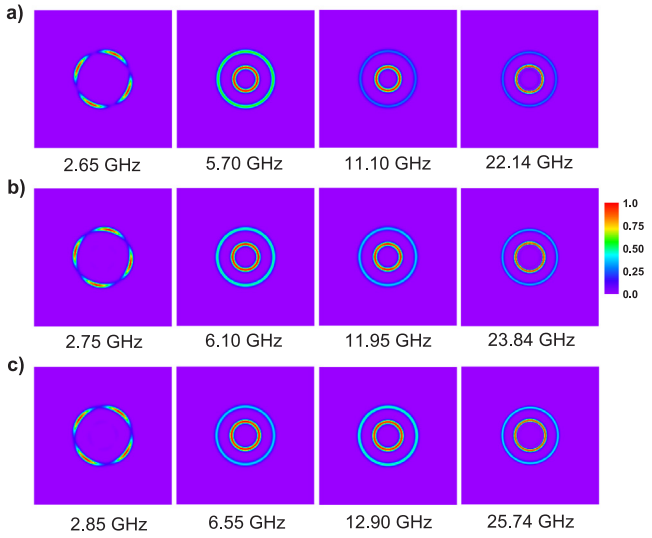

Fig. 3. Spatial distribution of the Fourier power of the spin wave modes 1, 2, 3 and 4, for (a) $D_{int} = 4.0$ mJ/m^2, (b) $D_{int} = 4.1$ mJ/m^2 and (c) $D_{int} = 4.2$ mJ/m^2.

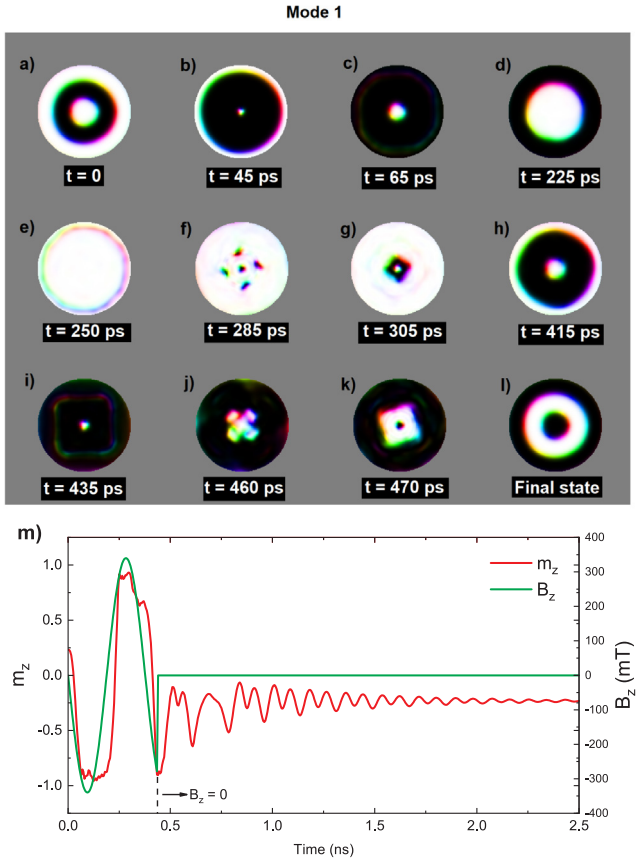

Fig. 4. (a-l) Images of the nanodisk exhibiting the spatial variation of the magnetization for different times, for Mode 1 (white color → $m_z = +1$, and black color → $m_z = -1$) for $D_{int} = 4.0$ mJ/m^2. Fig. 4 (m) shows the temporal evolution of the average z-component of the magnetization m_z and the field B_z.

with polarity $p = +1$ (Fig. 4 (a)), up to a skyrmionium with polarity $p = -1$ (Fig. 4 (l)). For this mode, we have encountered that the switching is possible for a magnetic field threshold of $B_0 = 340$ mT, pulse length of $t = 438$ ps[6].

During the application of the magnetic field, the inner region of the skyrmionium (in white) shrinks, and the outer region (also in white) also shrinks. The intermediate region (black) expands. These changes are shown in Fig. 4 (b). The intermediate region continues to expand up to the edges of the nanodisk, making the outer region disappear, and the inner region expands slightly, resulting in the formation of a skyrmion (Fig. 4 (c)). The core of this skyrmion ($p = +1$) continues to expand (Fig. 4 (d)) until the magnetization of the disk is saturated in the $+z$ direction (Fig. 4 (e)). Next, the magnetic configuration in the nanodisk evolves to the more complex magnetic configuration shown in Fig. 4 (f). This magnetic configuration, on its turn, evolves into another skyrmionium (Fig. 4 (g)). Next, the magnetic configuration evolves (Fig. 4 (h-i)) in a similar way to the evolution shown in Fig. 4(b-c). The temporal evolution of the system after turning off the magnetic field is shown in Fig. 4 (j-l), and it is possible to observe the magnetic configuration evolve to a deformed skyrmionium with polarity $p = -1$ (Fig. 4 (j-l)), until the skyrmionium is finally stabilized in the nanodisk (the complete switching process can be seen in video 1 in the Supplementary material).

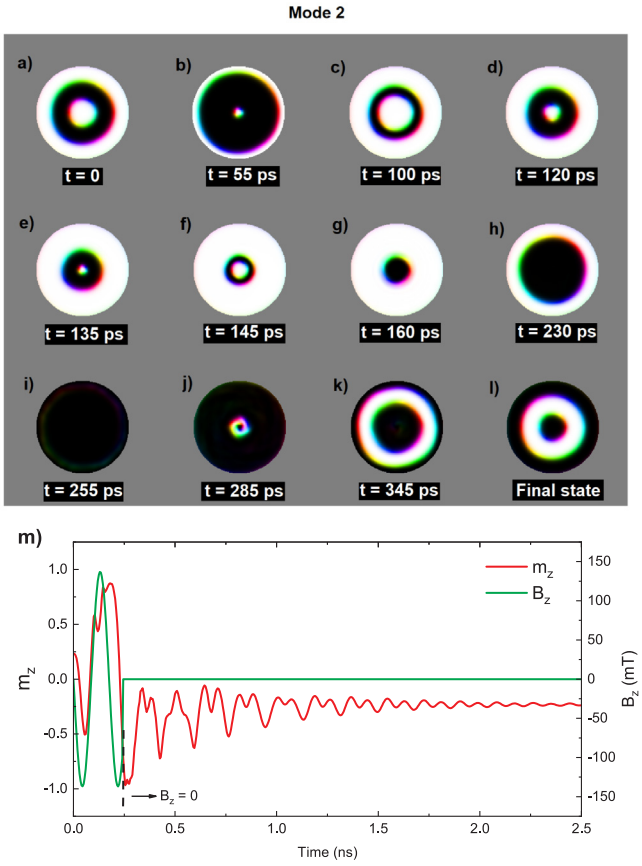

Fig. 5. (a-l) Images of the nanodisk exhibiting the spatial variation of the magnetization for different times, for Mode 2 (white color → $m_z = +1$, and black color → $m_z = -1$) for $D_{int} = 4.0$ mJ/m^2. Fig. 4 (m) shows the temporal evolution of the average z-component of the magnetization m_z and the field B_z.

In Fig. 5 it is shown the spatial evolution of the magnetization with time, and the temporal evolution of the average z-component of the magnetization m_z and B_z for mode 2. For this mode, we have encountered that the switching is possible for a threshold magnetic field intensity of $B_0 = 137$ mT, pulse length of $t = 242$ ps. The switching process of the skyrmionium is different from the one shown in Fig. 4.

[6] For practical reasons, we have considered the application of the oscillating fields for a maximum period of 1 ns. If in this period there was no switching, we increased the value of the magnetic field intensity.

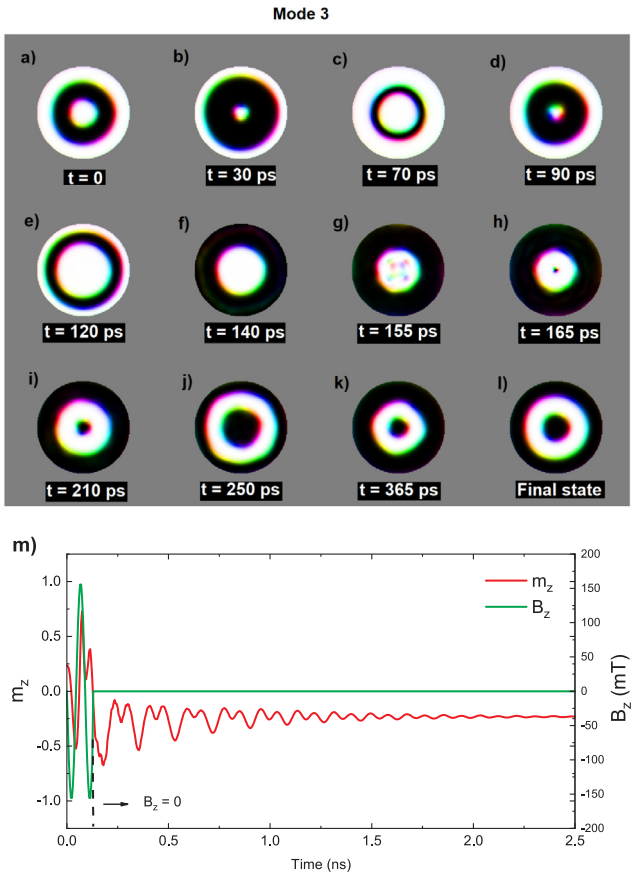

Fig. 6. (a-l) Images of the nanodisk exhibiting the spatial variation of the magnetization for different times, for Mode 3 (white color → $m_z = +1$, and black color → $m_z = -1$) for $D_{int} = 4.0$ mJ/m^2. Fig. 4 (m) shows the temporal evolution of the average z-component of the magnetization m_z and the field B_z.

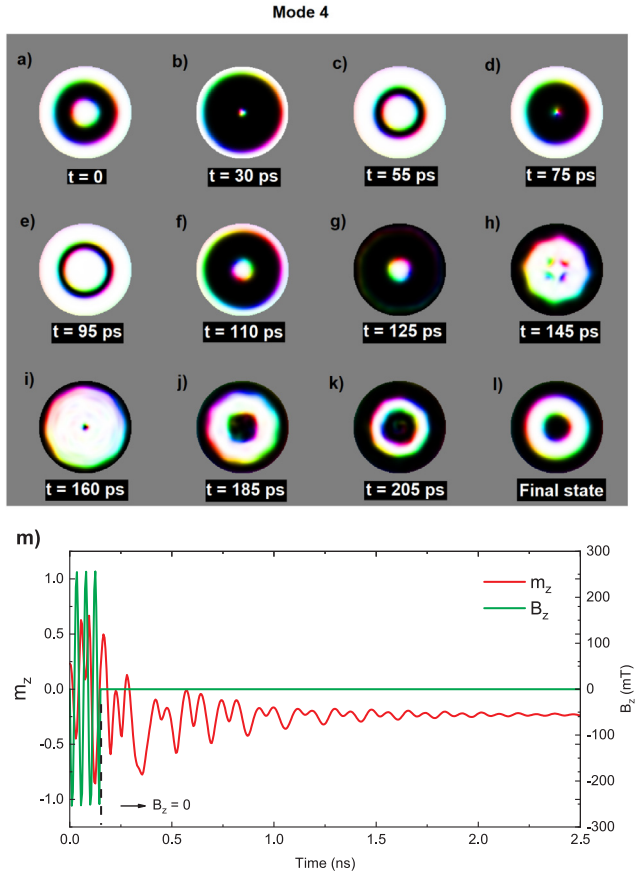

Fig. 7. (a-l) Images of the nanodisk exhibiting the spatial variation of the magnetization for different times, for Mode 4 (white color → $m_z = +1$, and black color → $m_z = -1$) for $D_{int} = 4.0$ mJ/m^2. Fig. 4 (m) shows the temporal evolution of the average z-component of the magnetization m_z and the field B_z.

For this mode, the inner region of the skyrmionium (in white) shrinks, and the outer region (also in white) also shrinks. The intermediate region (black) expands (Fig. 5 (b)). Then an opposite process occurs. The inner region of the skyrmionium (in white) expand, and the outer region (also in white) also shrinks. The intermediate region (black) expands. (Fig. 5 (c)). Next, the magnetic configuration in the nanodisk evolves in the same way as mentioned above (Fig. 5 (d-f)), until the inner region is annihilated and the skyrmionium is transformed into a skyrmion, as shown in Fig. 5 (g).

The core of the skyrmion expands, as shown in Fig. 5 (h). As mentioned above, the magnetic field is turned off at t = 242 ps, and the core of the skyrmion continues to expand to saturate the magnetization in the −z direction (Fig. 5 (i)). The magnetic configuration continues to evolve until a tiny skyrmionium appears at approximately t = 285 ps (Fig. 5 (j)). This skyrmionium expands and shrinks until it is finally stabilized on the nanodisk (Fig. 5 (l)). The complete switching process can be seen in video 2 in the Supplementary Material.

The switching process for mode 3 is shown in Fig. 6. In this figure, we can see that the evolution of the spatial distribution of the magnetization is similar to what is observed in the switching process for mode 2, at least until the formation of the skyrmion (Fig. 6 (a-f)).

In this case, the core of the skyrmion does not expand until the sample is saturated in the -z direction, as in the case for mode 2 (Fig. 5 (i)), but the core shrinks, and then a skyrmionium appears (Fig. 6 (h)). Then, the skyrmionium shrinks and expands, and it is finally stabilized on the nanodisk. For this mode, we have found that the switching is possible for a threshold magnetic field intensity of $B_0 = 158$ mT and pulse length of t = 129 ps. The complete switching process can be seen

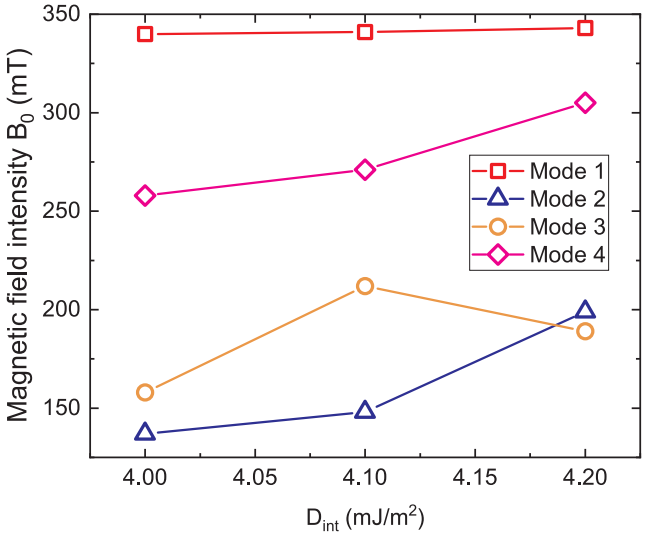

Fig. 8. Threshold magnetic field intensity B_0 versus D_{int}. Red squares for mode 1, blue triangles for mode 2, orange circles for mode 3, and purple diamonds for mode 4.

in video 3 in the Supplementary Material.

For mode 4, we have found that the switching is possible for a threshold magnetic field intensity of $B_0 = 258$ mT, pulse length of t = 146 ps. The spatial evolution of the magnetization with time, and

the temporal evolution of the average z-component of the magnetization m_z and B_z are shown in Fig. 7. This switching process is similar to that observed in mode 3. The complete switching process can be seen in video 4 in the Supplementary Material.

The similarity in the temporal evolution of the z-component of the magnetization, before the skyrmionium is switched, arises because mode 3 and mode 4 are similar, as shown in Fig. 3 (a). Mode 2 is somewhat different from mode 3 and mode 4, that is why there is a slight difference in the switching process. On the other hand, the switching process for mode 1 differs from all others, due to the way its Fourier power is distributed on the nanodisk (Fig. 3 (a)). Similar results were obtained for the other values of D_{int} shown in Fig. 1.

In Fig. 8 we show the value of the threshold magnetic field intensities B_0 as a function of the values of D_{int}, for all modes obtained, as shown in Fig. 3. In this figure we can observe that, in general, the increase of D_{int} leads to an increase in the values of the threshold magnetic field intensities B_0. For example, for mode 1, the threshold magnetic field intensity B_0 increases from B_0 = 340 mT (D_{int} = 4.0 mT) to B_0 = 343 mT (D_{int} = 4.2 mT). For mode 2, B_0 increases from B_0 = 137 mT (D_{int} = 4.0 mT) to B_0 = 199 mT (D_{int} = 4.2 mT), and for mode 4, B_0 increases from B_0 = 258 mT (D_{int} = 4.0 mT) to B_0 = 305 mT (D_{int} = 4.2 mT).

We found one exception for this behavior mentioned above; for mode 3, B_0 increases from B_0 = 158 mT (D_{int} = 4.0 mT) to B_0 = 212 mT (D_{int} = 4.1 mT) and then decreases to B_0 = 189 mT (D_{int} = 4.2 mT). This exception can be attributed to the intrinsic nonlinearity of the system.[7]

From Fig. 3 and Fig. 8, it is possible to observe that modes whose maximum oscillation amplitudes are closer to the center (mode 3, mode 4 and mode 5) allow the use of low intensity magnetic fields, compared to modes whose maximum oscillations are far from the center (mode 1). This is why it is important to know previously the distribution of the spin wave modes in order to use the lowest values of magnetic field intensity that are required for the practical applications.

3. Conclusions

In summary, in this work we have studied the switching process of a skyrmionium in a ferromagnetic nanodisk coupled to a nonmagnetic substrate, using micromagnetic simulation.

Our results show that perpendicular oscillating magnetic fields can be used to switch the polarity of a skyrmionium when the frequency of the magnetic fields is equal to the frequencies of the spin wave modes, and the magnetic field is turned off at the right time.

Our results show also that the switching process of a skyrmionium is mediated by a topological transformation before its reversal. The switching process show similarities in the case where the modes have similar spatial distributions.

Additionally, our results show that in general the increase of the values of D_{int} increases the value of the threshold magnetic field intensity necessary to induce the switching of a skyrmionium.

In the present work we have shown how, using the different resonance modes of the skyrmioniums, one can obtain a robust technique of manipulating the polarity of these structures, a requirement for many applications in Spintronics, where the two polarities would represent '0' or "1'. In the search for this technique, we have been able to reveal the full complexity of the process of polarity inversion of the skyrmioniums.

Credit authorship contribution statement

H. Vigo-Cotrina: Conceptualization, Methodology, Software, Writing - original draft. **A.P. Guimarães:** Supervision, Writing - review & editing, Resources.

Declaration of Competing Interest

The authors declare that they have no known competing financial interests or personal relationships that could have appeared to influence the work reported in this paper.

Acknowledgments

The authors would like to thank the support of the Brazilian agencies FAPERJ and CNPq. Additionally, we would like to thank Ing. H. Arteaga Chanduvi for providing us with the hardware for the completion of this work.

Appendix A. Supplementary data

Supplementary data associated with this article can be found, in the online version, athttps://doi.org/10.1016/j.jmmm.2020.166895.

References

[1] F. Garcia, H. Westfahl, J. Schoenmaker, E.J. Carvalho, A.D. Santos, M. Pojar, A.C. Seabra, R. Belkhou, A. Bendounan, E.R.P. Novais, A.P. Guimarães, Tailoring magnetic vortices in nanostructures, Appl. Phys. Lett. 97 (2) (2010) 022501, , https://doi.org/10.1063/1.3462305.
[2] J.-H. Kim, K.-S. Lee, H. Jung, D.-S. Han, S.-K. Kim, Information-signal-transfer rate and energy loss in coupled vortex-state networks, Appl. Phys. Lett. 101 (9) (2012) 092403, , https://doi.org/10.1063/1.4748885.
[3] S. Sugimoto, Y. Fukuma, S. Kasai, T. Kimura, A. Barman, Y. Otani, Dynamics of coupled vortices in a pair of ferromagnetic disks, Phys. Rev. Lett. 106 (2011) 197203, , https://doi.org/10.1103/PhysRevLett.106.197203.
[4] G. Siracusano, R. Tomasello, A. Giordano, V. Puliafito, B. Azzerboni, O. Ozatay, M. Carpentieri, G. Finocchio, Magnetic radial vortex stabilization and efficient manipulation driven by the Dzyaloshinskii-Moriya interaction and spin-transfer torque, Phys. Rev. Lett. 117 (2016) 087204, , https://doi.org/10.1103/PhysRevLett.117.087204.
[5] Y. Ma, C. Song, C. Jin, J. Wang, H. Xia, Y. Wei, J. Wang, Q. Liu, Microwave-driven dynamic switching of the radial vortex in a nanodot by micromagnetic simulation, J. Phys. D: Appl. Phys. 52 (19) (2019) 195001, , https://doi.org/10.1088/1361-6463/ab0356.
[6] R.V. Verba, D. Navas, A. Hierro-Rodriguez, S.A. Bunyaev, B.A. Ivanov, K.Y. Guslienko, G.N. Kakazei, Overcoming the limits of vortex formation in magnetic nanodots by coupling to antidot matrix, Phys. Rev. Appl. 10 (2018) 031002, , https://doi.org/10.1103/PhysRevApplied.10.031002.
[7] J. Sampaio, V. Cros, S. Rohart, A. Thiaville, A. Fert, Nucleation, stability and current-induced motion of isolated magnetic skyrmions in nanostructures, Nature Nanotechnol. 8 (2013) 839–844, https://doi.org/10.1038/nnano.2013.210.
[8] H.Y. Yuan, X.R. Wang, Skyrmion creation and manipulation by nano-second current pulses, Sci. Rep. 6 (2016) 22638, https://doi.org/10.1038/srep22638.
[9] S.-Z. Lin, C. Reichhardt, A. Saxena, Manipulation of skyrmions in nanodisks with a current pulse and skyrmion rectifier, Appl. Phys. Lett. 102 (22) (2013) 222405, , https://doi.org/10.1063/1.4809751.
[10] K.Y. Guslienko, Néel skyrmion stability in ultrathin circular magnetic nanodots, Appl. Phys. Express 11 (6) (2018) 063007, , https://doi.org/10.7567/APEX.11.063007.
[11] J.-V. Kim, F. Garcia-Sanchez, J.a. Sampaio, C. Moreau-Luchaire, V. Cros, A. Fert, Breathing modes of confined skyrmions in ultrathin magnetic dots, Phys. Rev. B 90 (2014) 064410, https://doi.org/10.1103/PhysRevB.90.064410.
[12] H. Vigo-Cotrina, A.P. Guimarães, Influence of the dipolar interaction in the creation of skyrmions in coupled nanodisks, J. Magn. Magn. Mater. 489 (2019) 165406, , https://doi.org/10.1016/j.jmmm.2019.165406.
[13] A.C. Booth, Y. Liu, J. Zang, Collective modes of three-dimensional magnetic structures: a study of target skyrmions, J. Magn. Magn. Mater. 489 (2019) 165447, , https://doi.org/10.1016/j.jmmm.2019.165447.
[14] X. Zhang, J. Xia, Y. Zhou, D. Wang, X. Liu, W. Zhao, M. Ezawa, Control and manipulation of a magnetic skyrmionium in nanostructures, Phys. Rev. B 94 (2016) 094420, , https://doi.org/10.1103/PhysRevB.94.094420.
[15] F. Zheng, H. Li, S. Wang, D. Song, C. Jin, W. Wei, A. Kovács, J. Zang, M. Tian, Y. Zhang, H. Du, R.E. Dunin-Borkowski, Direct imaging of a zero-field target skyrmion and its polarity switch in a chiral magnetic nanodisk, Phys. Rev. Lett. 119 (2017) 197205, , https://doi.org/10.1103/PhysRevLett.119.197205.
[16] S. Li, J. Xia, X. Zhang, M. Ezawa, W. Kang, X. Liu, Y. Zhou, W. Zhao, Dynamics of a magnetic skyrmionium driven by spin waves, Appl. Phys. Lett. 112 (14) (2018) 142404, , https://doi.org/10.1063/1.5026632.
[17] C. Song, C. Jin, J. Wang, Y. Ma, H. Xia, J. Wang, J. Wang, Q. Liu, Dynamics of a magnetic skyrmionium in an anisotropy gradient, Appl. Phys. Express 12 (8) (2019) 083003, , https://doi.org/10.7567/1882-0786/ab30d8.
[18] H. Vigo-Cotrina, A.P. Guimarães, Creating skyrmions and skyrmioniums using

[7] Similar behaviors were obtained for a nanodisk with thickness L = 0.4 nm (see Supplementary Material).

oscillating perpendicular magnetic fields, J. Magn. Magn. Mater. 507 (2020) 166848, , https://doi.org/10.1016/j.jmmm.2020.166848.
[19] A. Bogdanov, A. Hubert, The stability of vortex-like structures in uniaxial ferromagnets, J. Magn. Magn. Mater. 195 (1) (1999) 182–192, https://doi.org/10.1016/S0304-8853(98)01038-5.
[20] G. Finocchio, F. Büttner, R. Tomasello, M. Carpentieri, M. Kläui, Magnetic skyrmions: from fundamental to applications, J. Phys. D: Appl. Phys. 49 (42) (2016) 423001, , https://doi.org/10.1088/0022-3727/49/42/423001.
[21] X. Zhao, C. Jin, C. Wang, H. Du, J. Zang, M. Tian, R. Che, Y. Zhang, Direct imaging of magnetic field-driven transitions of skyrmion cluster states in FeGe nanodisks, PNAS 113 (18) (2016) 4918–4923, https://doi.org/10.1073/pnas.1600197113.
[22] S. Zhang, J. Wang, Q. Zheng, Q. Zhu, X. Liu, S. Chen, C. Jin, Q. Liu, C. Jia, D. Xue, Current-induced magnetic skyrmions oscillator, New J. Phys. 17 (2) (2015) 023061, , https://doi.org/10.1088/1367-2630/17/2/023061.
[23] C. Wang, D. Xiao, X. Chen, Y. Zhou, Y. Liu, Manipulating and trapping skyrmions by magnetic field gradients, New J. Phys. 19 (8) (2017) 083008, , https://doi.org/10.1088/1367-2630/aa7812.
[24] A.G. Kolesnikov, M.E. Stebliy, A.S. Samardak, A.V. Ognev, Skyrmionium – high velocity without the skyrmion Hall effect, Sci. Rep. 8 (2018) 16966, https://doi.org/10.1038/s41598-018-34934-2.
[25] B. Göbel, A.F. Schäffer, J. Berakdar, I. Mertig, S.S.P. Parkin, Electrical writing, deleting, reading, and moving of magnetic skyrmioniums in a racetrack device, Sci. Rep. 9 (2019) 12119, https://doi.org/10.1038/s41598-019-48617-z.
[26] X. Zhang, M. Ezawa, Y. Zhou, Magnetic skyrmion logic gates: conversion, duplication and merging of skyrmions, Sci. Rep. 5 (2015) 9400, https://doi.org/10.1038/srep09400.
[27] R. Tomasello, E. Martinez, R. Zivieri, L. Torres, M. Carpentieri, G. Finocchio, A strategy for the design of skyrmion racetrack memories, Sci. Rep. 4 (2014) 6784, https://doi.org/10.1038/srep06784.
[28] J. Müller, Magnetic skyrmions on a two-lane racetrack, New J. Phys. 19 (2) (2017) 025002, , https://doi.org/10.1088/1367-2630/aa5b55.
[29] B. Zhang, W. Wang, M. Beg, H. Fangohr, W. Kuch, Microwave-induced dynamic switching of magnetic skyrmion cores in nanodots, Appl. Phys. Lett. 106 (10) (2015) 102401, , https://doi.org/10.1063/1.4914496.
[30] C. Heo, N.S. Kiselev, A.K. Nandy, S. Blügel, T. Rasing, Switching of chiral magnetic skyrmions by picosecond magnetic field pulses via transient topological states, Sci. Rep. 6 (2016) 27146, https://doi.org/10.1038/srep27146.
[31] D. Bhattacharya, M.M. Al-Rashid, J. Atulasimha, Energy efficient and fast reversal of a fixed skyrmion two-terminal memory with spin current assisted by voltage controlled magnetic anisotropy, Nanotechnology 28 (42) (2017) 425201, , https://doi.org/10.1088/1361-6528/aa811d.
[32] J. Wang, C. Jin, C. Song, H. Xia, J. Wang, Q. Liu, Rapid creation and reversal of skyrmion in spin-valve nanopillars, J. Magn. Magn. Mater. 474 (2019) 472–476, https://doi.org/10.1016/j.jmmm.2018.11.036.
[33] S. Abdizadeh, J. Abouie, K. Zakeri, Dynamical switching of confined magnetic skyrmions under circular magnetic fields, Phys. Rev. B 101 (2020) 024409, , https://doi.org/10.1103/PhysRevB.101.024409.
[34] A. Vansteenkiste, J. Leliaert, M. Dvornik, M. Helsen, F. Garcia-Sanchez, B. Van Waeyenberge, The design and verification of Mumax3, AIP Adv. 4 (10) (2014) 107133, , https://doi.org/10.1063/1.4899186.
[35] X. Liu, Q. Zhu, S. Zhang, Q. Liu, J. Wang, Static property and current-driven precession of 2π)vortex in nanodisk with Dzyaloshinskii-Moriya interaction, AIP Adv. 5 (8) (2015) 087137, , https://doi.org/10.1063/1.4928727.